Liquid Crystals
Publication details, including instructions for authors and subscription information:
http://www.informaworld.com/smpp/title~content=t713926090

Electric field-driven director oscillations in nematic liquid crystals

Geoffrey R. Luckhurst[a]; Akihiko Sugimura[b]; Bakir A. Timimi[a]
[a] School of Chemistry and Southampton Liquid Crystal Institute, University of Southampton, Highfield, Southampton SO17 1BJ, United Kingdom [b] Department of Information Systems Engineering, Osaka Sangyo University, Daito, Osaka 574-8530, Japan

To cite this Article Luckhurst, Geoffrey R. , Sugimura, Akihiko and Timimi, Bakir A.(2005) 'Electric field-driven director oscillations in nematic liquid crystals', Liquid Crystals, 32: 11, 1449 — 1463
To link to this Article: DOI: 10.1080/02678290500191352
URL: http://dx.doi.org/10.1080/02678290500191352

Liquid Crystals, Vol. 32, No. 11–12, November–December 2005, 1449–1463

Electric field-driven director oscillations in nematic liquid crystals

GEOFFREY R. LUCKHURST†, AKIHIKO SUGIMURA‡ and BAKIR A. TIMIMI*†

†School of Chemistry and Southampton Liquid Crystal Institute, University of Southampton, Highfield, Southampton SO17 1BJ, United Kingdom

‡Department of Information Systems Engineering, Osaka Sangyo University, 3-1-1 Nakagaito, Daito, Osaka 574-8530, Japan

(*Received 13 February 2005; accepted 9 May 2005*)

We have used deuterium NMR spectroscopy to investigate the director dynamics and equilibrium behaviour in nematic liquid crystals (4-pentyl- and 4-octyl-4′-cyanobiphenyl, (5CB and 8CB), both specifically deuteriated) when subject to magnetic and a.c. electric fields. The angle between the magnetic and electric fields can be varied between 0 and 90° and the most common geometry we have used is for an angle of about 45°. For 5CB and 8CB (with positive $\Delta\tilde{\chi}$ and $\Delta\tilde{\varepsilon}$) the director orientation was measured using time-resolved NMR both when the electric field is applied and when it is turned off. In all cases it was found that the director alignment was uniform and the director relaxation follows closely the predictions of the torque-balance equation given by the Leslie–Ericksen theory. In all these experiments we have employed a 10 kHz electric field; at such a relatively high frequency the director experiences an effectively constant value of the electric field. We have now investigated the behaviour of the nematic director for the two liquid crystals at much lower frequencies of the electric field: several Hz to about 1000 Hz. As before, the director orientation was measured using time-resolved deuterium NMR spectroscopy. We have employed two geometries. In one, the electric and magnetic fields were inclined at ~50°. We found that the director oscillates between two extreme orientations (determined by the frequency and the field strength) in a plane formed by the magnetic and electric fields. The oscillations were observed to continue for many cycles, indicating that the coherence in the director orientation was not lost during this motion. The director was found to remain uniformly aligned. The two extreme director orientations can also be determined from the NMR spectrum time-averaged over many thousands of cycles of oscillations. At low frequencies (several Hz) these limiting angles are essentially independent of frequency but as the frequency increases so the two angles approach each other and become equal at high frequencies. More recently, we have used a geometry with the angle between the fields of ~90°. A threshold behaviour is observed in this geometry for the director orientation as a function of the applied voltage. The time-averaged spectra at low frequencies and at certain voltages showed unusual powder-like features. Time-resolved NMR measurements at 40 Hz and different voltages near the threshold value were carried out to understand the oscillatory behaviour which was also simulated. Turn-on and turn-off dynamics at high frequency were conducted revealing intriguing differences between the two pathways for the field-induced relaxation. These results will be discussed and interpreted in terms of the torque-balance equation with a time dependent electric field.

1. Introduction

The dynamic response of a uniform nematic director to changing external electric and magnetic fields is controlled by a number of material physical properties namely the dielectric anisotropy, $\Delta\tilde{\varepsilon}$, the diamagnetic anisotropy, $\Delta\tilde{\chi}$, the rotational viscosity coefficient, γ_1, as well as by the strength of the applied fields and the angle between them. The viscosity coefficient is especially important in determining the response times of nematic liquid crystal display devices. The rotational viscosity coefficient can be determined by a method in which the orientation of the director with respect to the magnetic field is suddenly changed and the return of the director to its equilibrium orientation is monitored using, for example [1–3], deuterium NMR.

The time-resolved NMR experiment has been extended by using an electric field both to create the original non-equilibrium state of the system and to drive the director [3–7]. For a uniformly aligned director

*Corresponding author. Email: B.A.Timimi@soton.ac.uk

Liquid Crystals
ISSN 0267-8292 print/ISSN 1366-5855 online © 2005 Taylor & Francis
http://www.tandf.co.uk/journals
DOI: 10.1080/02678290500191352

subject to both electric and magnetic fields, the dynamics of the changes in the director orientation relative to the magnetic field direction, θ, are given, within the framework of the Leslie–Ericksen hydrodynamic theory, by the torque-balance equation [3]

$$\gamma_1(\mathrm{d}\theta/\mathrm{d}t) = -\left(\mu_0^{-1}\Delta\tilde{\chi}\mathrm{B}^2/2\right)\sin 2\theta + \left(\varepsilon_0\Delta\tilde{\varepsilon}\mathrm{E}^2/2\right)\sin 2(\alpha-\theta). \quad (1)$$

Here α is the angle between the magnetic and electric fields, μ_0 is the magnetic constant, B is the magnetic flux density, E is the electric field and ε_0 is the vacuum permittivity.

When the electric field is switched on, and provided $\Delta\tilde{\varepsilon}$ is positive, the director orientation is predicted to change according to

$$\tan[\theta(t)-\theta_\infty] = \tan(\theta_0-\theta_\infty)\exp(-t/\tau_\mathrm{C}). \quad (2)$$

Here, θ_0 is the initial director orientation, θ_∞ is its final equilibrium orientation and the composite relaxation time, τ_C, is given by

$$\tau_\mathrm{C} = \left(\tau_\mathrm{M}^{-2} + 2\tau_\mathrm{M}^{-1}\tau_\mathrm{E}^{-1}\cos 2\alpha + \tau_\mathrm{E}^{-2}\right)^{-1/2}, \quad (3)$$

where τ_E is the relaxation time for the pure electric field-induced motion of the director given by

$$\tau_\mathrm{E} = \gamma_1/\varepsilon_0\Delta\tilde{\varepsilon}\,\mathrm{E}^2 \quad (4)$$

and τ_M is the analogous magnetic relaxation time given by

$$\tau_\mathrm{M} = \gamma_1\mu_0/\Delta\tilde{\chi}\,\mathrm{B}^2. \quad (5)$$

When the electric field is switched off, and provided $\Delta\tilde{\chi}$ is positive, the director orientation now varies according to

$$\tan\theta(t) = \tan\theta_0\exp(-t/\tau_\mathrm{M}). \quad (6)$$

The experiments combining both electric and magnetic fields have the advantage that the ratio of the anisotropic susceptibilities, $\Delta\tilde{\varepsilon}/\Delta\tilde{\chi}$, is readily measured from the equilibrium state, that is when the director orientation attains the value of θ_∞ as a result of keeping the electric field continuously on. By measuring the relaxation times, the rotational viscosity coefficient can be determined provided the value of either $\Delta\tilde{\varepsilon}$ or $\Delta\tilde{\chi}$ is available independently from other experiments [3, 8]. The other advantage of using the electric field in NMR is that by changing the electric field strength and/or the angle α, we can change the relaxation time τ_C—see equations (3) and (4)—and so extend the range of conditions for the relaxation experiments. In contrast, the magnetic flux density of modern spectrometers is fixed and so, for any given temperature, we have no control over the value of τ_M.

The director dynamics, according to the torque-balance equation (1), also depends on the angle between the electric and magnetic fields. In the experimental geometry we have used we are able to change the value α continuously between 0 and 90°. The importance of being able to adjust the value of α is that it makes it possible to choose between two distinct geometries. In the first geometry the two fields are orthogonal to each other. Here, there is a degeneracy in the way the director can move from its initial to its final equilibrium orientation, hence the director alignment process can proceed through a non-uniform director distribution before reaching the equilibrium state [9–11]. In the second geometry, the two fields are at an angle of $\leqslant 45°$ to each other and there is now no degeneracy; hence this geometry provides a unique path for the director allowing it to remain uniformly aligned during the relaxation process [1–7]. For values of α between 45° and 90°, theory predicts that a mixture of the uniform and non-uniform relaxation pathways should occur (see the appendix). In our work on the field-induced director alignment in the presence of the two fields we have employed both geometries, with some intriguing results as we shall show later.

In order to measure the relaxation times, τ_M and τ_C, we need, according to equations (2) and (6), to follow the time dependence of the angle $\theta(t)$. We have used deuterium NMR spectroscopy to monitor $\theta(t)$ utilizing the simple dependence of the liquid crystal deuterium NMR spectrum on the angle between the director and **B**. For a uniformly aligned nematic containing a group of equivalent deuterons, the deuterium NMR spectrum consists of a single quadrupolar doublet, provided any dipolar couplings are negligible. One of the advantages of using NMR spectroscopy in investigating director dynamics is that the quadrupolar splitting, $\Delta\tilde{\nu}$, depends on the angle θ according to

$$\Delta\tilde{\nu}(\theta) = \Delta\tilde{\nu}_0 P_2(\cos\theta). \quad (7)$$

Here, $\Delta\tilde{\nu}_0$ is the quadrupolar splitting when the director is parallel to **B** and $P_2(\cos\theta)$ is the second Legendre function. In our experimental investigations we have employed a high frequency electric field, typically several kHz, to ensure that disruption of the director orientation by conductive motion of ions is eliminated [3]. In this case, the electric field in the torque-balance equation (1) is taken to be constant (equal to V_RMS). Clearly the periodic variation in the square of the electric field will, under certain conditions, influence the director dynamics; thus as the electric field increases so the relaxation time given by equation (3) will decrease

caused by a reduction in τ_E, and as the field decreases so τ_C will increase caused by an increase in τ_E. In addition, the direction of the director alignment will be reversed when the electric field starts to decrease; however the precise moment when this occurs will depend on the frequency of the electric field in comparison with the composite relaxation rate, τ_C^{-1}. The importance of these variations in the electric field to the validity of the analysis, based on the assumption that the electric field is constant, will also depend on the frequency of the electric field and the composite relaxation rate for the director. Here, we review briefly the results of our investigations obtained using a high frequency electric field, and then consider the question of using low frequency electric fields both theoretically and experimentally. Some of the results at low frequencies obtained using two basic experimental geometries in which the value of θ_∞ is $<45^\circ$ [7] and $\sim 90^\circ$ will be given. As we shall also see, considerations at low frequency electric fields have led us to a novel variation in the NMR method used to study field-induced director dynamics and hence determine certain nematic properties [7].

2. Experimental

The liquid crystals used in our studies were the mesogens 4-α,α-d_2-pentyl-4′-cyanobiphenyl (5CB-d_2) (T_{NI}=307.5 K) [12] and 4-α,α-d_2-octyl-4′-cyanobiphenyl (8CB-d_2) which has a nematic and a smectic A phase (T_{NI}=312.1 K and T_{SmAN}=304.7 K) [13]. Both of these liquid crystals are deuteriated in the α-position of the alkyl chain and both have positive $\Delta\tilde{\varepsilon}$ and $\Delta\tilde{\chi}$ values. This deuteriation pattern gives us the simplest deuterium NMR spectrum. As we shall find, the deuterium NMR spectrum of a monodomain of 5CB-d_2 and 8CB-d_2 contains the expected single quadrupolar doublet. The liquid crystal samples were contained in cells composed of two glass slides each coated with indium oxide to form the electrodes and varying in thickness between 50 and 100 μm. The surfaces of the electrodes were not treated in any way and so the surface anchoring strength was of the order of 10^{-7} J m^{-2}, corresponding to weak anchoring [14]. The sinusoidal electric field was produced using a function generator, Wave Factory WF1943, NF Electronic Instruments, and a high power amplifier, model 4005 NF Electronic Instruments.

The deuterium NMR spectra were measured using a JEOL Lambda 300 spectrometer which has a magnetic flux density of 7.05 T. A quadrupolar echo sequence, sketched in figure 1, was used to record the free induction decay (FID) which, after averaging, was Fourier-transformed to obtain the conventional

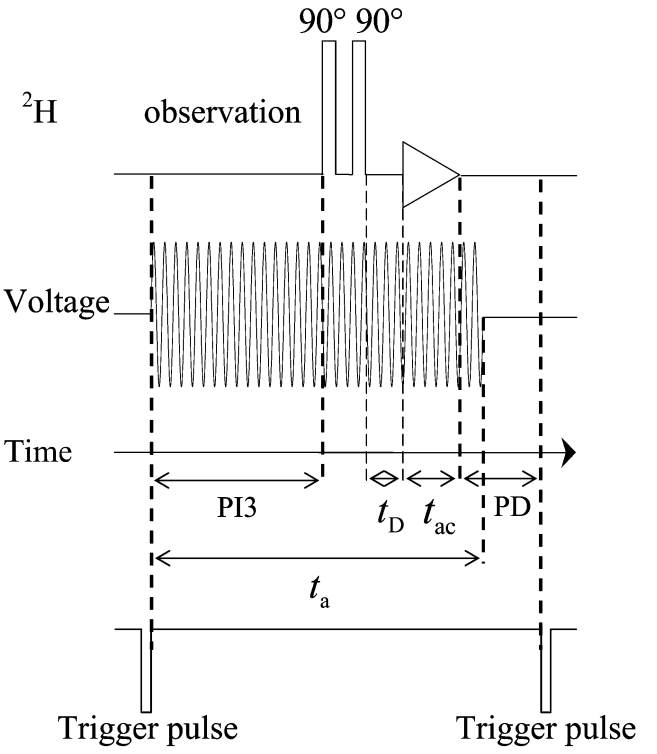

Figure 1. The pulse train for the time-resolved measurements. The trigger pulse from the spectrometer initializes one FID measurement: it switches **E** on; after a time PI3 one FID is acquired during t_{ac} following the quadrupolar echo pulse sequence; the electric field is turned off after time t_a; finally after a delay time PD the next trigger pulse initialiates another FID measurement cycle.

frequency domain spectrum; also shown in this figure is the sinusoidal electric field pulse. For the turn-on experiments, this field was applied for a time, t_a, corresponding to an integer number of electric field oscillations, and finishing after the FID acquisition was complete. The dead time of the receiver coil, t_D, was about 10 μs, the time between pulses was 40 μs, each pulse was 7.5 μs long, the acquisition time for the FID was about 1 ms and finally the delay time, PD, was given values in the range 50 to 200 ms with the longer times being used at the lower frequencies. This delay allows the director to be realigned parallel to the magnetic field following the removal of the electric field and, incidentally, allows the deuterium spins time to relax back to their equilibrium distribution. The experiment was performed by activating a trigger pulse from the spectrometer to switch on the electric field; at the same time the trigger pulse initiates the pulse sequence to measure a single FID. The time at which the measurement takes place, following the application of the field, is controlled by the interval PI3 (see figure 1) although the total time to the acquisition of the FID is

the sum of PI3, the dead time, the time between pulses and the acquisition time. The second trigger pulse shown in the figure initiates another complete cycle allowing the FIDs to be averaged before Fourier transformation to give the spectrum. To obtain spectra with a good signal-to-noise ratio depends on the cell thickness, the natural spectral linewidths and spectral line broadening caused by the spread in the director orientation; sometimes tens of thousands of FIDs were typically averaged. For the turn-off experiments, the same pulse sequences shown in figure 1 were used except now the FID was acquired after the electric field is turned off.

3. Dynamics at several kHz electric field

We have used high frequency electric fields utilizing the pulse sequences shown in figure 1 to investigate the equilibrium director distribution as well as the dynamics of its alignment in the turn-on and turn-off modes for the nematic phase of specifically deuteriated 5CB and 8CB [3, 4, 6, 12, 15]. In these investigations the experimental geometry was carefully chosen so that the angle between the electric and magnetic field as well as the electric field strength are such as to ensure that the director follows a uniform relaxation pathway. In figure 2 we show some typical time-resolved spectra for 5CB-d_2 at 295 K [4]. The spectra consist of the anticipated quadrupolar doublet indicative of a uniform director distribution (monodomain) throughout the relaxation process. In the turn-on process, the quadrupolar splitting decreases and saturates with time after $\sim$3 ms. In the turn-off process, the quadrupolar splitting increases with time as the director moves towards the magnetic field and becomes parallel to it after $\sim$3 ms. The spectra shown in figure 2 contain weak oscillatory spectral features associated with the director rotation during the acquisition time for the FID [16]. When these oscillations are on the inside of the main spectral peaks they indicate that the director is moving away from the magnetic field; when they are on the outside of the main peaks they indicate that the director is moving towards the magnetic field [16]. The presence of these weak spectral oscillatory features does not affect the final analysis of the time dependence of $\theta(t)$. The time variations of the director orientation at any given time, $\theta(t)$, for the turn-on and turn-off processes was found to fit equations (2) and (6), respectively, very well in all the cases investigated. As an example we show in figure 3 the best fits for 8CB-d_2 [6]. As can be seen, the fits are indeed very good confirming that the alignment pathway for this geometry is uniform and that the dynamics of changes in the director orientation follows the torque-balance equation based on the Leslie–Ericksen

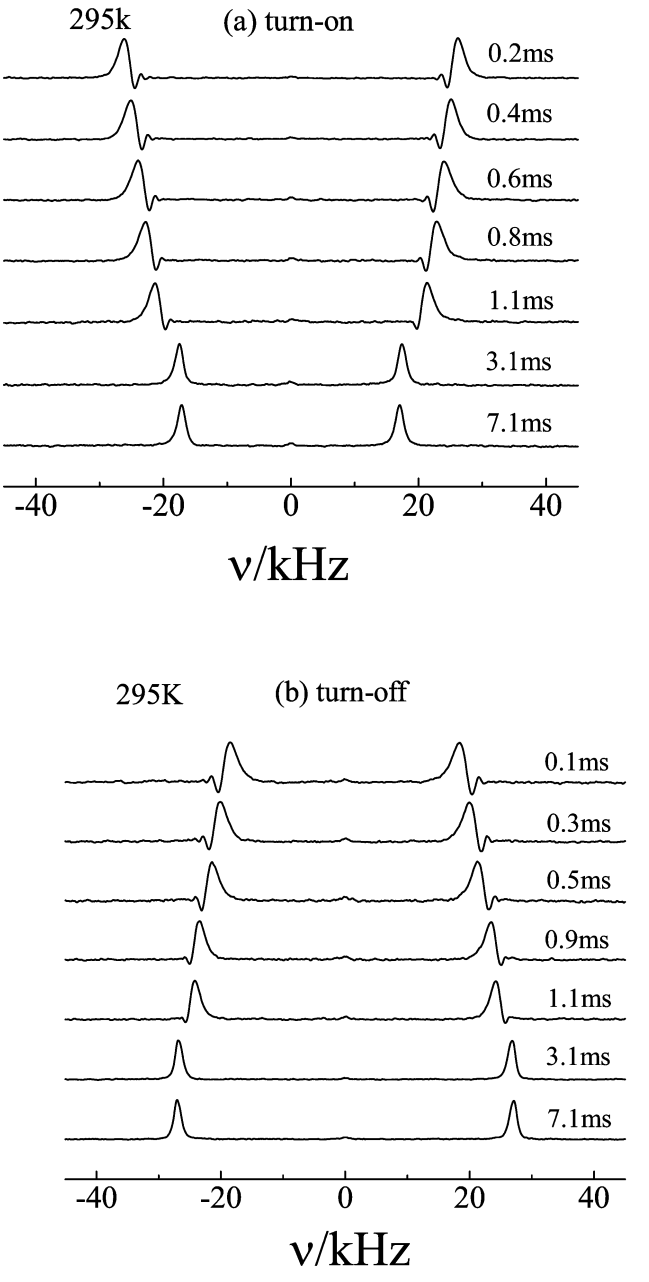

Figure 2. Time-resolved deuterium NMR spectra measured during the director alignment of 5CB-d_2 in the nematic phase at 295 K for a 56.1 μm cell at $V=50$ V and $\alpha\approx45^\circ$. (*a*) Typical turn-on relaxation spectra, $\theta_\infty=30^\circ$; (*b*) typical turn-off relaxation spectra from $\theta_0=30^\circ$ [4].

hydrodynamic theory, see equation (1). Equations (2) and (6) describe very well the uniform relaxation of the director in the nematic phase over a wide range of temperatures and values of α. For 5CB, for example, the dynamic measurements covered the temperature range 0°C to the nematic–isotropic transition at 35.5°C [4, 5]. Equations (2) and (6) were also found to be valid for all molecular sites of the nematogen used to monitor the

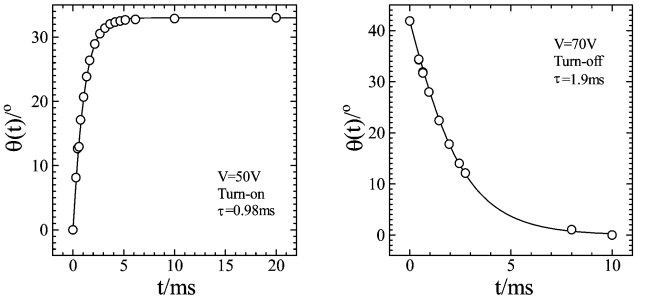

Figure 3. The time variation of $\theta(t)$ for the turn-on, at 308 K, and turn-off, at 306 K, processes for 8CB-d_2. The solid lines are the best fits calculated according to equations (2) and (6), respectively [6].

relaxation processes and to yield the same relaxation time for all these molecular sites [5]. Furthermore, the measurement of the turn-on and turn-off relaxation times from the dynamic experiments, combined with the equilibrium measurement of the director orientation when the electric field is applied continuously, offered a reliable method of obtaining the material properties: $\Delta\tilde{\varepsilon}/\Delta\tilde{\chi}$, $\gamma_1/\Delta\tilde{\chi}$ or $\gamma_1/\Delta\tilde{\varepsilon}$ [4]. In particular, when the electric field is applied continuously and the director attains its equilibrium orientation θ_∞, the left hand side of equation (1) will be zero and so we find [4]

$$\left(\frac{\Delta\tilde{\chi}}{\Delta\tilde{\varepsilon}}\right)=\frac{\mathrm{E}^2\varepsilon_0\mu_0}{\mathrm{B}^2}. \tag{8}$$

It should be pointed out here that **E** is the RMS value.

From the measurement of the equilibrium director orientation with the electric field we obtain θ_∞ and from equation (8) the ratio of the material parameters $(\Delta\tilde{\chi}/\Delta\tilde{\varepsilon})$ is then obtained (see [17]). Knowing either of $\Delta\tilde{\chi}$ or $\Delta\tilde{\varepsilon}$ we can then determine the rotational viscosity coefficient, γ_1, from, for example, the measurement of τ_M and equation (5). We have used this procedure to determine the values of γ_1 at different temperatures [4, 6] utilizing the published values of $\Delta\tilde{\varepsilon}$ [18].

4. Dynamics at low frequency electric fields

4.1. *Theoretical considerations*

The key consideration for the low frequency (in the sense that the reciprocal of the frequency is greater than the composite director relaxation time) case is to replace E^2 in the torque-balance equation by the time-dependent sinusoidal expression

$$\mathrm{E}^2=\mathrm{E}_0^2\sin^2 2\pi ft, \tag{9}$$

where f is the frequency of the sinusoidal electric field. The torque-balance equation can then be written in the following form using generalized or scaled co-ordinates [7]

$$\begin{aligned}\mathrm{d}\theta/\mathrm{d}t^* = &-(1/2)\sin 2\theta\\ &+(\rho/2)\sin^2(2\pi f*t^*)\sin 2(\alpha-\theta).\end{aligned} \tag{10}$$

In this equation

$$t^*=t/\tau_\mathrm{M}, \tag{11}$$

$$f^*=f\Big/\tau_\mathrm{M}^{-1} \tag{12}$$

and the parameter ρ is the ratio of electric to magnetic anisotropic energies

$$\rho=\mu_0\varepsilon_0\frac{\mathbf{E}_0^2}{\mathbf{B}^2}\left(\frac{\Delta\tilde{\varepsilon}}{\Delta\tilde{\chi}}\right) \tag{13}$$

which depends, therefore, on the material property $\Delta\tilde{\varepsilon}/\Delta\tilde{\chi}$ and the experimental parameter E_0/B. For a given value of α, the time dependence of the director orientation will be determined by ρ and the scaled frequency, f^*. An analytical solution to the time-dependent generalized equation could not be found and so the equation was solved numerically [7]. Figure 4 shows the results of these calculations for α equal to 44.7°. The ratio ρ used was 3.47 which is typical of 5CB and the field strengths employed in our experiments. As can be seen from figure 4 for the highest value of f^* of 15.4, the director orientation $\theta(t)$ increases smoothly from zero and then levels off. The time variation of the director orientation is, apart from extremely weak oscillations superimposed on this curve [7], indistinguishable from that given by equation (2) based on the

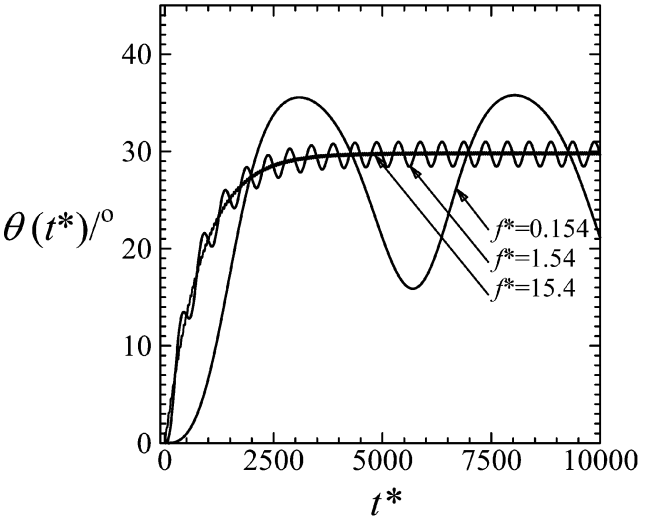

Figure 4. The scaled time dependence of the angle made by the director with the magnetic field, $\theta(t^*)$, calculated with $\alpha=44.7°$ and $\rho=3.47$ for f^* equal to 15.4, 1.54 and 0.154 [7].

torque-balance equation, equation (1), in which E is a constant. However, when f^* is reduced by a factor of ten to 1.54 the magnitude of the oscillations has grown significantly and these are now clearly visible. We find that the frequency of the oscillations is equal to that of the square of the electric field although the director orientation exhibits a phase lag with respect to the electric field. Of more interest is the fact that the director is predicted to rotate through an angle greater than that expected at high frequencies, when the director experiences the root mean square field. This occurs because the slower rate of change in the electric field allows the director a greater opportunity to respond to the higher electric field, E_0. As the scaled frequency is further reduced by a factor of 10 to 0.154, the oscillatory motion of the director is now very large indeed. The maximum director orientation has increased significantly and the reduction in the minimum orientation is even larger. As the rate of change in E^2 is slowed the director is able to follow the electric field more closely and will approach the limiting value of θ_{max} given by [7]

$$\cos 2\theta^0_{max} = (1+\rho\cos 2\alpha)\Big/\left(1+2\rho\cos 2\alpha+\rho^2\right)^{1/2}, \quad (14)$$

where the superscript zero indicates the maximum value at zero frequency; by analogy the minimum angle at zero frequency should be denoted by θ^0_{min} and here this is zero. For f^* of 0.154, θ^0_{min} is not reached because the relaxation time is too long to enable the director to follow the electric field instantaneously. Only at much lower frequencies of the electric field, for example at $f^*=0.0154$, would θ^0_{min} reach the value of zero [7]. Also the calculations at longer times predict that the director oscillations continue unattenuated indefinitely. The calculations further show that the director oscillations, after several cycles, achieve a quasi-equilibrium or stationary state when the values of θ_{max} and θ_{min} no longer vary with time. In this limit, it is found that the difference between θ_{max} and θ_{min} changes with frequency as shown in figure 5. Since this scaled frequency depends on the magnetic relaxation time the values of θ_{max} and θ_{min}, therefore, contain information concerning the field-induced dynamics. This is a very interesting result as it offers a new, indirect route, via time-averaged NMR as we shall see later, to study the field-induced director dynamics. As we can see from figure 5, as f^* tends to zero, both θ_{max} and θ_{min} reach their limiting values and become constant. At high frequency both angles approach, in a non-symmetric way, the limiting high frequency value of θ_∞ In between the low and high frequency limits, the values of θ_{max} and θ_{min}, at intermediate values of f^* will be

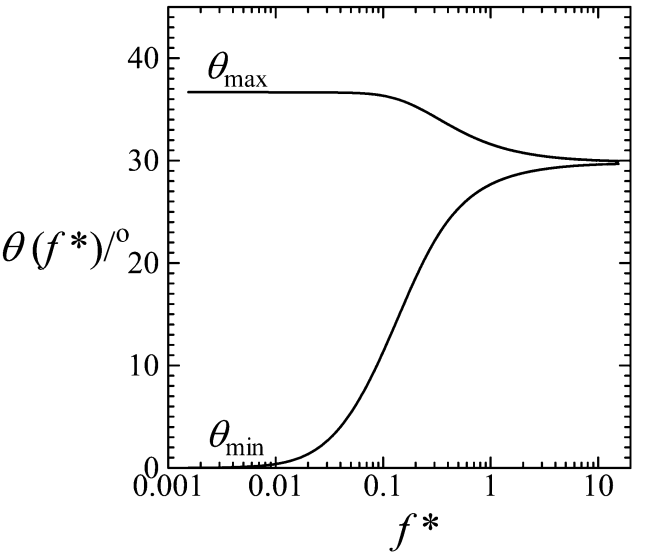

Figure 5. The scaled frequency dependence, shown on a logarithmic scale, of θ_{max} and θ_{min} predicted for a system with $\alpha=44.7^\circ$ and $\rho=3.47$.

determined by the director dynamics, i.e. τ_M, as well as by ρ and α.

4.2. *Results for α≈50°*

We have measured the time-resolved and time-averaged deuterium NMR spectra at a range of low frequencies in order to verify the predictions described in §4.1. We show typical time-resolved spectra in figure 6 for 5CB-d_2 at 295 K, E_0 was 1.26 MV m^{-1} and f was 100 Hz [7]; these clearly indicate the oscillations in the quadrupolar splittings. In figure 7 we show $\theta(t)$, obtained from the time-resolved spectra, as a function of time. Figure 7 also shows the simulated curve as well as the time variation in E^2. The oscillation in the director orientation at 100 Hz is very clear. The simulated curve is calculated with τ_M equal to 1.54 ms (see [4]), ρ of 3.45 and the value of α set equal to the experimental value of 44.7°. Incidentally, figure 7 also shows the phase lag between E^2 and the director orientation $\theta(t)$. The overall agreement between the simulated curve based on this set of parameters and the experimental values is very good, as is clearly apparent from the comparison in figure 7. We have also studied the same sample cell for a significantly longer time. The results show that the oscillations in $\theta(t)$ extend over many cycles without any indication of attenuation and that at longer times the oscillations reach a steady state so that values of θ_{min} and θ_{max} level off. The prediction of the time dependence of $\theta(t)$ based on the hydrodynamic theory, see equation (10), for longer times was found to be in very good agreement with the experimental results,

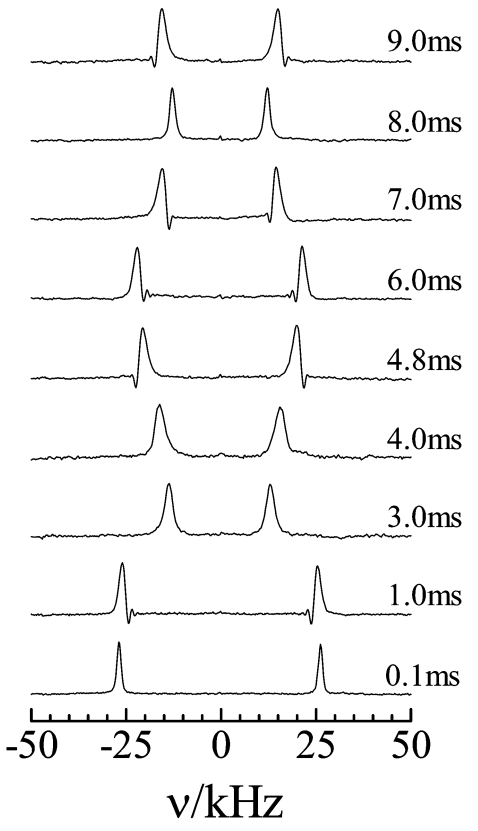

Figure 6. The time dependence of the deuterium NMR spectrum of 5CB-d_2 recorded at 295 K with an a.c. electric field of 100 Hz for different values of time following the application of an electric field of strength 1.26 MV m^{-1}.

providing strong support for the validity of the analysis, the parameters and the experiment [7].

The director oscillations are predicted to increase in magnitude with decreasing frequency (see figure 4). We have confirmed this by carrying out time-resolved NMR measurements at the very low frequency of 10 Hz for the electric field for just over the first cycle. The experimental data for the time dependence of the director orientation agrees quite well with the prediction of the hydrodynamic theory [7]. Because the motion of the director is higher than the rate of change of the electric field at such a low frequency, it was found that the director remains parallel not to the field itself but to the effective field resulting from the combination of the electric and magnetic fields [7].

We turn now to the results obtained for the time-averaged spectra determined at different frequencies. These spectra show how the director distribution is affected by the oscillations induced by the low frequency electric fields. The time-averaged spectra are normally obtained by switching the a.c. electric field on and leaving it on while tens of thousands of FIDs are

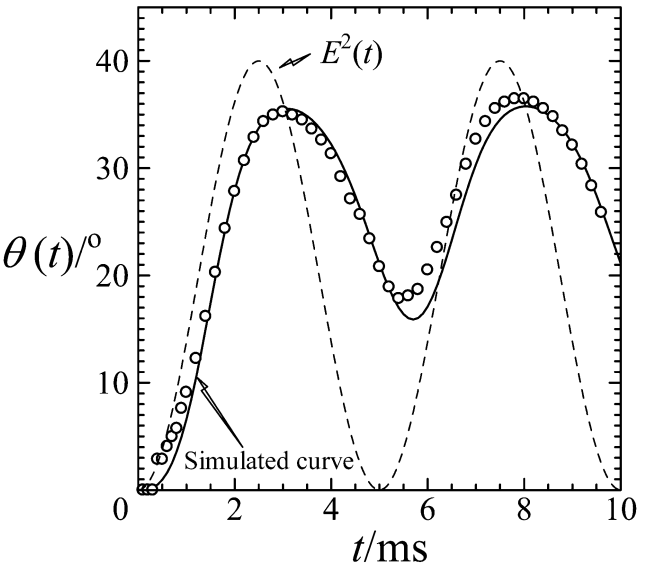

Figure 7. The time dependence of $\theta(t)$ determined for 5CB-d_2 at 295 K, with an a.c. electric field of 100 Hz and strength of 1.26 MV m^{-1}. The solid line was calculated with ρ=3.45, τ_M=1.54 ms and α=44.7°. The dashed line shows the time dependence of $\mathbf{E}^2$.

acquired. Figure 8 shows such time-averaged spectra for 5CB-d_2 at 288 K and for a range of frequencies from 1000 to 10 Hz. It is apparent that, instead of a single quadrupolar doublet expected for a monodomain nematic at high frequency, there are two doublets with spectral intensity between them. This indicates that the director adopts a range of orientations, extending from θ_{min} to θ_{max} corresponding to the range $\Delta\tilde{\nu}_{max}$ to $\Delta\tilde{\nu}_{min}$ during the application of the electric field, see equation (7). A time-averaged spectrum can be understood as the sum of the time-resolved spectra over one cycle of director orientations during the stationary state of director oscillations. We have also simulated the time-averaged spectrum for 5CB-d_2 at 10 Hz and 288 K by dividing one cycle of director oscillation, for the steady state of oscillations, into a very large number of discrete time values, calculating the time-resolved spectrum for each of these discrete time values and then summing all the time-resolved spectra for such a cycle. The agreement with experiment was found to be very good which provides additional support for the validity of the theory to evaluate the time dependence of the director orientation. It also suggests that the director oscillations continue unattenuated for the several thousand oscillations involved in measuring the time-averaged spectra [7].

In figure 8 we see that at the lowest frequency of the electric field the spectral extent is significant, corresponding to the large oscillations in the angle made by the director with the magnetic field. As the frequency of

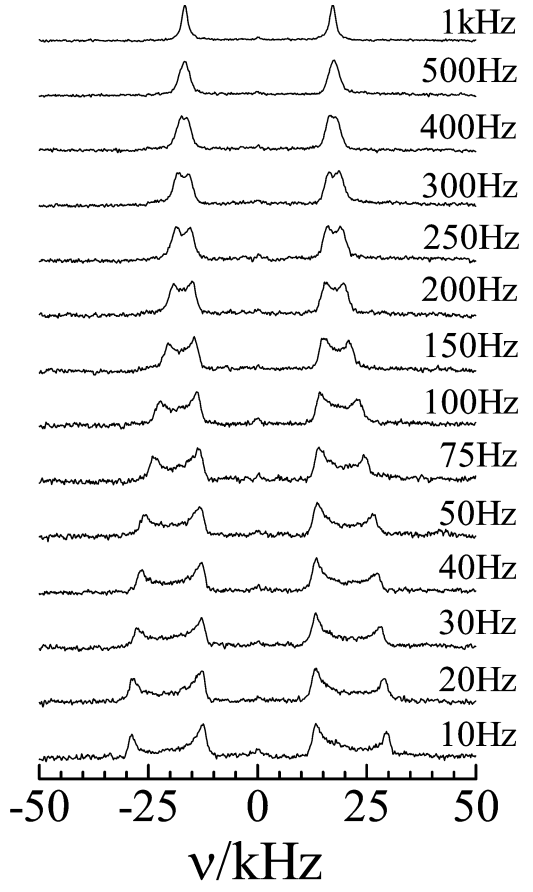

Figure 8. The time-averaged spectra for 5CB-d_2 measured for values of the frequency, between 10 Hz and 1 kHz, of the a.c. electric field with E_0 of 1.41 MV m^{-1} at 288 K.

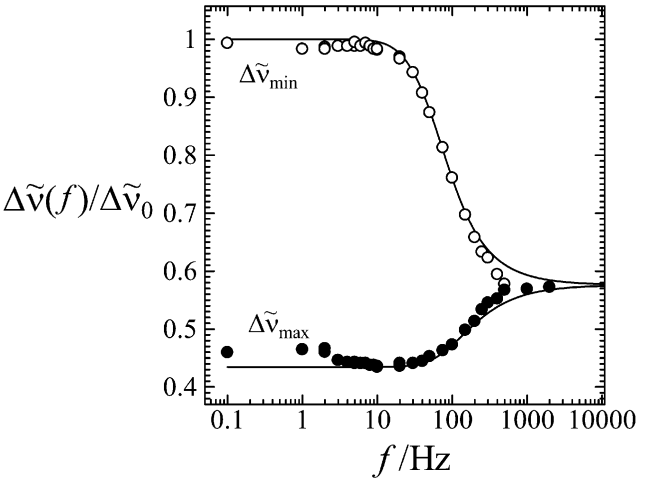

Figure 9. The limiting quadrupolar splittings $\Delta\tilde{\nu}_{max}(\equiv\theta_{min})$ and $\Delta\tilde{\nu}_{min}(\equiv\theta_{max})$ scaled with $\Delta\tilde{\nu}_0$ for 5CB-d_2 at 288 K as a function of frequency (logarithmic scale) determined from the time-averaged spectra. The solid line is calculated with ρ=4.37, τ_M=2.6 ms determined previously and α=44.7° [7].

the electric field is increased the oscillations in the director orientation are reduced in magnitude and with this the extent of the spectrum. At higher frequencies the spectral width decreases still further until the two doublets collapse to a single doublet, indicating that the director adopts a unique orientation, in accord with the analysis presented in figure 4. The values of the two extreme quadrupolar splittings, which can be estimated directly from the time-averaged spectrum, are plotted, scaled to $\Delta\tilde{\nu}_0$, as a function of frequency in figure 9. This presentation is in preference to plotting θ_{min} and θ_{max} as a function of frequency because of the large errors in the value of θ_{min} extracted from the quadrupolar splittings when the director is close to the magnetic field (see [7]). The predicted frequency dependence of the splittings is shown as the solid line in figure 9 and the agreement with the experimental values is clearly very good. By measuring time-averaged NMR spectra at different frequencies (which is technically an easier NMR experiment to perform than the time-resolved experiment) we obtain a new route to certain material properties of the nematic, namely, $\gamma_1/\Delta\tilde{\chi}$. It should be noted here that real dynamic information can be obtained only from the portion of figure 5 (or figure 9) where significant changes in the values of the extreme director orientations with frequency occur.

4.3. *Results for α≈90°*

In this section we discuss some recent measurements in which the geometry of the experiment was changed so that the electric field is very close to being orthogonal to the magnetic field, i.e. $\alpha\approx90°$. With this geometry the possibility exists of degenerate routes for the director to follow when it is aligned during a turn-on or turn-off alignment process. The liquid crystal we have used in these measurements is 8CB-d_2 in the nematic phase. This liquid crystal, which has a smectic A phase, was chosen in order to compare its behaviour with that of the nematic liquid crystal 5CB used in the earlier investigation.

For this unique geometry, and for the weak anchoring condition we use, we expect, in contrast to the behaviour for $\alpha\approx50°$, the director orientation θ to show initially no change as we increase the value of V_{RMS} and then to increase sharply as we approach a *threshold-like* voltage. Above this threshold voltage the director orientation is expected to saturate to near 90°. We show in figure 10 the results for the variation of the director orientation with voltage using an electric field of 5 kHz applied to a 100.6 μm cell containing 8CB-d_2

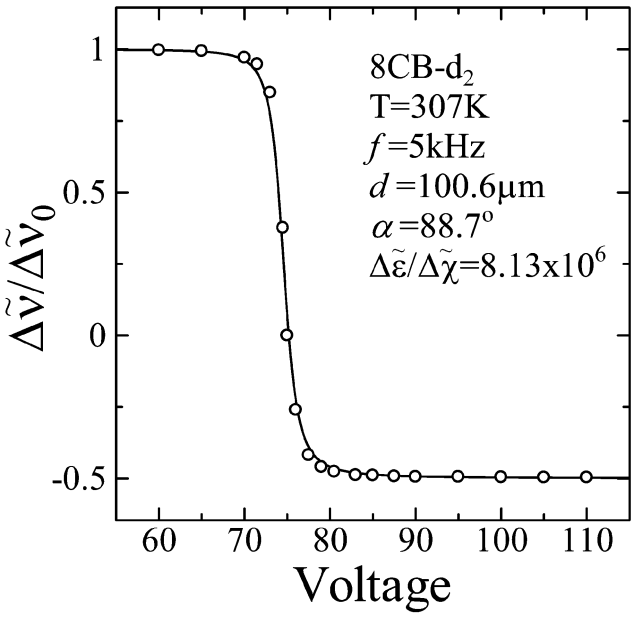

Figure 10. The variation of the quadrupolar splitting ratio, $\Delta\tilde{\nu}/\Delta\tilde{\nu}_0$, with the voltage applied to a 100.6 μm cell containing 8CB-d_2 at 307 K. The frequency of the applied electric field is 5 kHz and $\alpha = 88.7^\circ$, the solid line is calculated from equation (15) (see text).

in the nematic phase at 307 K. In figure 10, instead of plotting the director orientation θ, we plot the equivalent quantity, the experimentally measured ratio $\Delta\tilde{\nu}/\Delta\tilde{\nu}_0$, see equation (7). The quadrupolar splitting is seen to be essentially constant until the voltage reaches about 70 V when it begins to change. At this point the director orientation changes sharply from being nearly parallel to the magnetic field to nearly parallel to the electric field as the voltage changes from ~72 to ~77 V. The threshold voltage, taken as the midpoint on the sharply changing portion of the plot, is ~75 V. The individual experimental points in figure 10 correspond to the equilibrium orientation θ_∞, which can be written in terms of the variable ρ and the angle α as [3, 7]

$$\cos 2\theta_\infty = (2 + \rho\cos 2\alpha) \Big/ \left(4 + 4\rho\cos 2\alpha + \rho^2\right)^{1/2}. \qquad (15)$$

The solid line in figure 10 is fitted to equation (15) with $\alpha = 88.7^\circ$ and the material parameter $\Delta\tilde{\varepsilon}/\Delta\tilde{\chi} = 8.13 \times 10^6$. As we are using measurements covering the widest range in the equilibrium director orientation θ_∞, employing this geometry could, in principle, provide us with an accurate method of determining the material ratio $\Delta\tilde{\varepsilon}/\Delta\tilde{\chi}$. A better method, however, would be to measure the variation in θ_∞ with ρ for a range of values of α from ~50° to ~90° and use equation (15) to fit the data and so find the optimum value of $\Delta\tilde{\varepsilon}/\Delta\tilde{\chi}$ [17].

4.4. *Time-averaged NMR spectra at low frequencies*

We consider first the time-averaged behaviour of the nematic director when the cell is subject to low frequency electric fields. We show in figure 11 some typical time-averaged spectra at different voltages and frequencies. Here the situation in the presence of the threshold behaviour is more complicated than the case when α is considerably smaller than 90°. Inspection of the spectra in figure 11 shows that the values of both voltage and the (low) frequency have a drastic effect on the time-averaged spectra. It has to be remembered that these time-averaged spectra are in fact averages of the

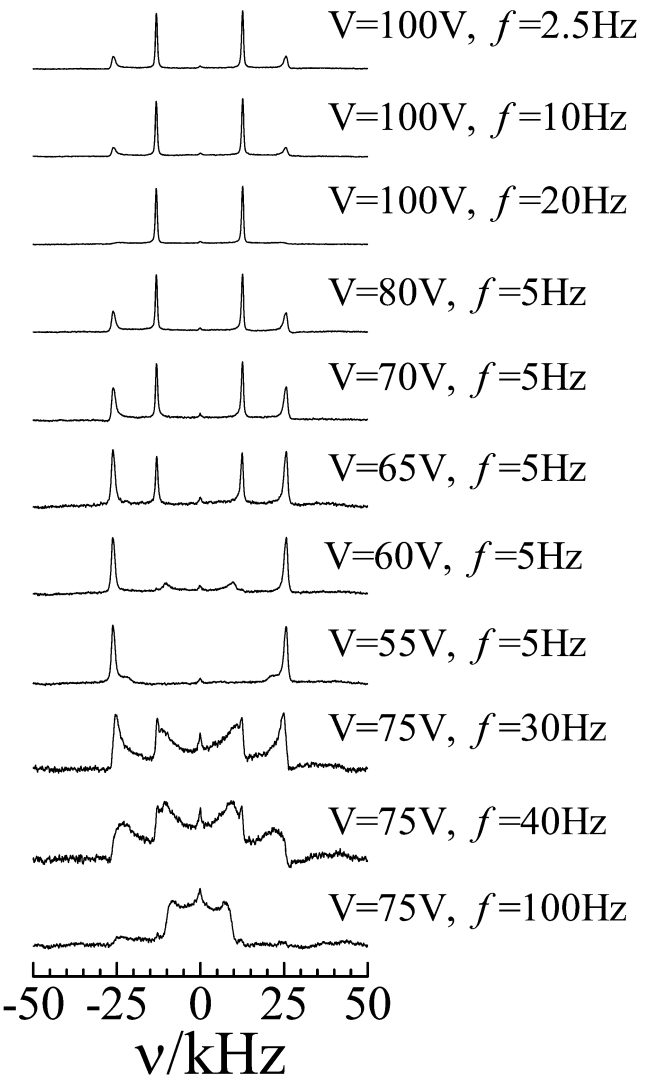

Figure 11. Time-averaged spectra at different voltages and low frequencies for the nematic phase of 8CB-d_2 in a 100.5 μm cell at 307 K and with $\alpha = 88.7^\circ$.

time-resolved spectra resulting from the dynamic director oscillations produced by the low frequency sinusoidal electric field in competition with the static magnetic field. We can interpret the spectra shown in figure 11 at a qualitative level in the following way. For frequencies of 20 Hz and below and voltages of 65 V and above, the spectra are characterized by the presence of two sets of quadrupolar splittings corresponding to the lower and higher values observed in the threshold plot of figure 10 (i.e. corresponding to θ_∞ values of 0 and $\sim 90^\circ$). The director spends its time proportionally either at $\theta_\infty \sim 0^\circ$ or $\theta_\infty \sim 90^\circ$. For the lower voltages of 60 and 55 V, the director now resides most of the time at $\theta_\infty \sim 0^\circ$. For electric fields with frequencies of 30 to 100 Hz and a voltage close to the threshold value, the situation appears more complex. The spectra in figure 11 at 75 V and 30, 40 and 100 Hz exhibit considerable complexity (with powder-like spectral features) and this suggests that during its oscillations the director may be residing most of the time in the threshold region. The quantitative interpretation of these time-averaged spectra requires the measurement and simulation of the time-resolved spectra at different voltages and frequencies. In the next section we present a selection of such measurements at one frequency (40 Hz) and two values of the voltage (75 and 77.5 V) close to its threshold value.

4.5. *Dynamics at 40 Hz*

Because of the complex time-averaged spectra we have observed at 'intermediate' frequencies and the threshold voltage (see figure 11) we chose to investigate the dynamics of the director oscillations at 40 Hz and at the threshold voltage of $75\,V_{RMS}$ and close to it at $77.5\,V_{RMS}$. We wanted to know if the powder-like spectral features of the time-averaged spectrum at $V=75$ V and 40 Hz are caused by the time-averaging of powder-like spectra from a non-uniform time-resolved director distribution or from a uniform time-resolved spectrum associated with a director distribution covering a wide range of orientations. We show in figure 12 some typical time-resolved spectra found for an electric potential of 75 V and at 40 Hz. It is clear that the time-resolved spectra are for an essentially uniform director distribution. The spectral lines in the doublet at 16 ms are sharp with a large splitting corresponding to a director orientation close to the magnetic field, see equation (7). The splitting decreases after 18 ms with some line broadening. This trend continues until at 21 and 22 ms the doublet collapses into essentially a single line at the magic angle. Then the splitting starts to increase, as the director orientation, $\theta(t)$, decreases, until at 26 ms the splitting is almost as large as it was at

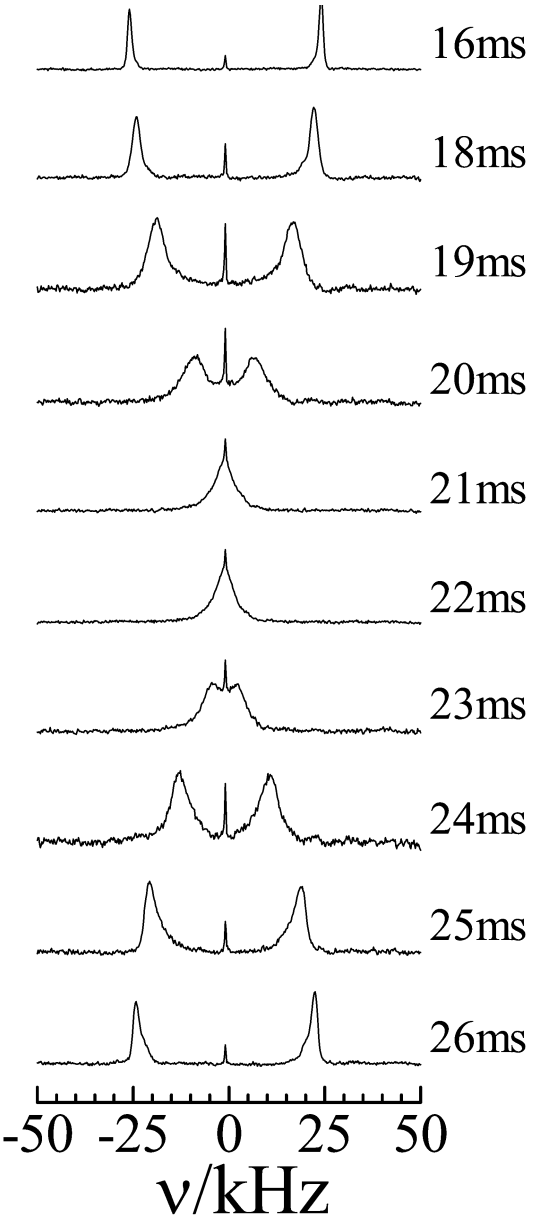

Figure 12. Time-resolved spectra for 8CB-d_2 at 307 K in the nematic phase during the director oscillation using a voltage of 75 V and 40 Hz frequency electric field applied to a 100.6 μm cell and for $\alpha=88.7^\circ$.

18 ms and we notice here also that there is some line broadening indicative of a small spread in the director orientation.

In figure 13 we show some typical time-resolved spectra for the director alignment but now for a slightly larger electric potential of 77.5 V at the same frequency. The spectra exhibit some line broadening similar to, but perhaps smaller than, that observed in the spectra in figure 12. Another interesting feature displayed by the spectra is the pattern of changes in the splitting between

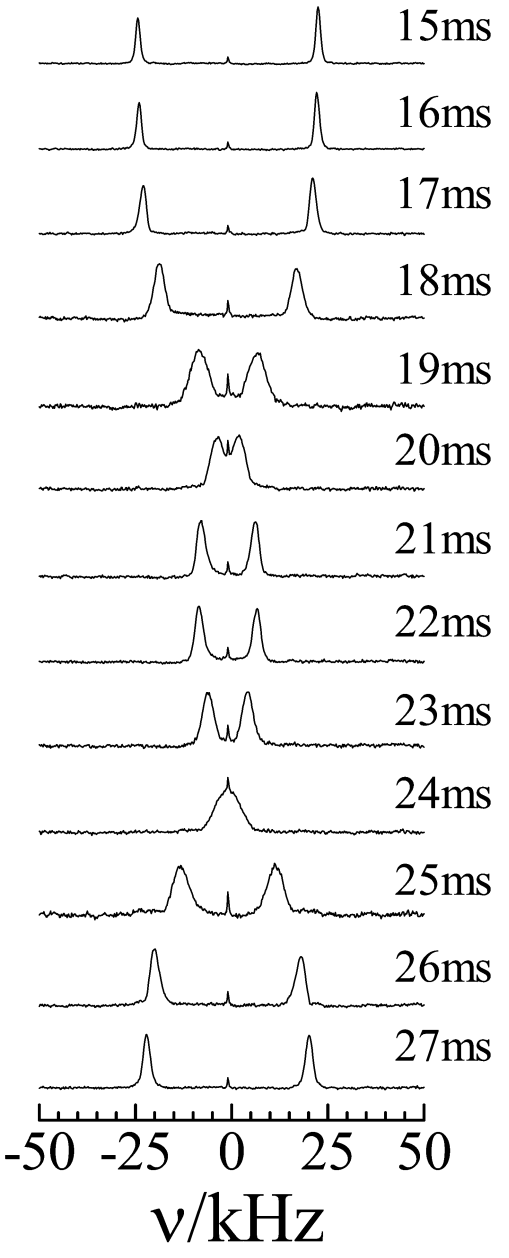

Figure 13. Time-resolved spectra for 8CB-d_2 at 307 K in the nematic phase during the director oscillation using a voltage of 77.5 V and 40 Hz frequency electric field applied to a 100.6 μm cell and for $\alpha=88.7^\circ$.

15 and 23 ms in which this decreases continuously between 15 and 20 ms, then increases to some extent between 20 and 22 ms. This pattern of change in the splitting is consistent with the director making a small angle of $\sim 7.5^\circ$ with the magnetic field at 15 ms, and then this angle increases continuously until it is about 70° at 22 ms. At times greater than 22 ms the angle starts to decrease continuously in the next part of the director oscillation cycle. The full oscillation pattern of the director is shown in figure 14 in which the ratio, $\Delta\tilde{\nu}/\Delta\tilde{\nu}_0$, is plotted against time for $V=75$ and 77.5 V. The oscillation is shallow for the first cycle and becomes deeper and deeper for the subsequent cycles and eventually these oscillations reach a steady state after

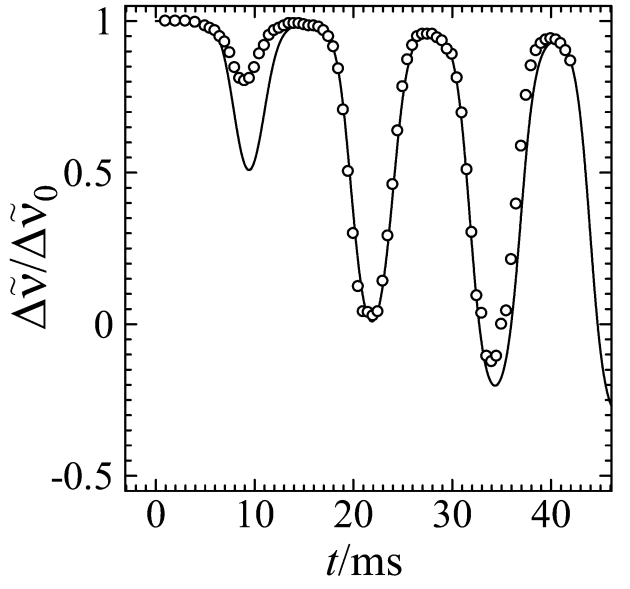

(*a*)

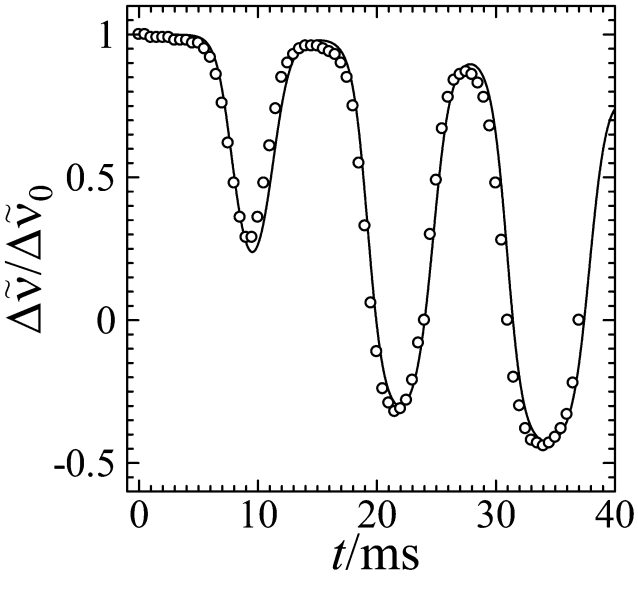

(*b*)

Figure 14. The change in the quadrupolar splitting ratio ($\Delta\tilde{\nu}/\Delta\tilde{\nu}_0$) with time, showing the director oscillations for 8CB-d_2 at 307 K in the nematic phase using a 40 Hz frequency electric field applied to a 100.6 μm cell and for $\alpha=88.7^\circ$. Circles are the experimental points and the solid line shows the predicted result. For (*a*) a voltage of 75 V and for (*b*) a slightly higher voltage of 77.5 V.

about 5 or 6 cycles [19]. The solid lines in figure 14 show the simulated behaviour based on the hydrodynamic theory, equation (10), and the value of ρ obtained from the ratio $(\Delta\tilde{\varepsilon}/\Delta\tilde{\chi}) = 8.13 \times 10^6$ found in fitting the data given in figure 10 and the value of τ_M determined in a previous study [6]. In figure 14 (*a*) the agreement with theory appears good for the second and third cycles of the oscillations but not so impressive for the first cycle where experimentally it is much shallower than predicted. However, the agreement between theory and experiment for the oscillations at $V = 77.5$ V shown in figure 14 (*b*) is on the whole very good. At the moment we are unable to account for the discrepancy shown in figure 14(*a*) at short times.

When $\alpha \approx 90^\circ$ we expect the director to relax in the turn-on or turn-off dynamics by following degenerate pathways of alignment which would cause the director distribution to become non-uniform. This should be apparent from the observation of powder-like deuterium NMR spectra sometime during the director alignment process. However, in the oscillation experiments we have just described, which could be thought of as a turn-on and a turn-off process during the rise and fall in the value of the electric field, the spectra we have measured were essentially monodomain spectra indicative of a uniform director distribution for the alignment at 40 Hz. Because of this surprising result it is important to investigate the behaviour under other conditions and so we have performed full turn-on and turn-off dynamics measurements for this geometry but now with a high frequency electric field.

5. Turn-on and turn-off dynamics at 5 kHz and $\alpha = 88.7^\circ$

5.1. *Turn-on dynamics*

The director orientation here is parallel to the magnetic field prior to the application of the electric field and the start of the turn-on time-resolved dynamics measurements as described in § 2. In figure 15 we show some typical turn-on time-resolved spectra obtained for 8CB-d_2 at 307 K in a 100.6 µm cell subject to a voltage of 84 V and 5 kHz frequency electric field. The value of the voltage was chosen to ensure that it is sufficiently large to align the director close to 88.7° (see figure 10). Most surprisingly, the time-resolved spectra show a monodomain director alignment from $\theta(t) = 0^\circ$ at $t = 0$ all the way to $\theta(t) \sim 85^\circ$ at $t = 50$ ms. Hence, in this experiment we observe the director following a uniform alignment relaxation pathway. In fact, we were able to fit the time dependence of the quadrupolar splitting ratio, $\Delta\tilde{\nu}/\Delta\tilde{\nu}_0$, to equation (2) perfectly with $\tau_C = 7.02$ ms and $\theta_\infty = 84.8^\circ$, as shown in figure 16.

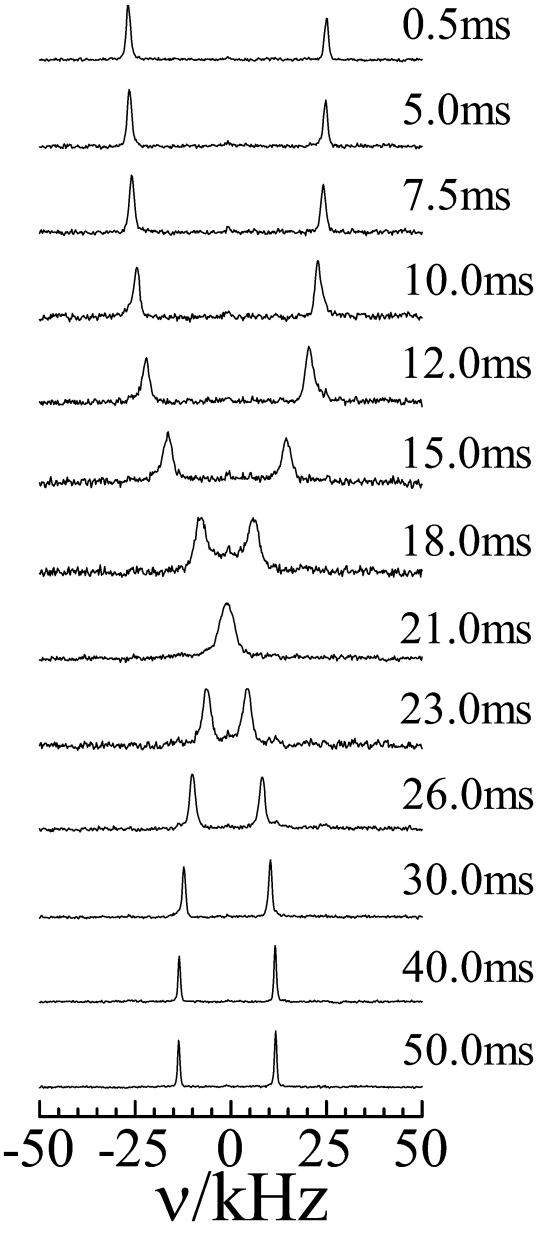

Figure 15. Time-resolved deuterium NMR spectra for the turn-on relaxation of 8CB-d_2 in the nematic phase at 307 K using a voltage of 84 V and 5 kHz frequency electric field applied to a 100.6 µm cell and for $\alpha = 88.7^\circ$

5.2. *Turn-off dynamics*

In this experiment, the electric field is applied to the cell to ensure an initial director orientation close to 90° before it is removed to start a time-resolved turn-off dynamics measurement as described in § 2. In figure 17 (*a*) we show some typical time-resolved spectra for the turn-off dynamics obtained for 8CB-d_2 at 307 K and for $\alpha = 88.7^\circ$. It is immediately apparent from the spectra in figure 17 (*a*) that during the turn-off

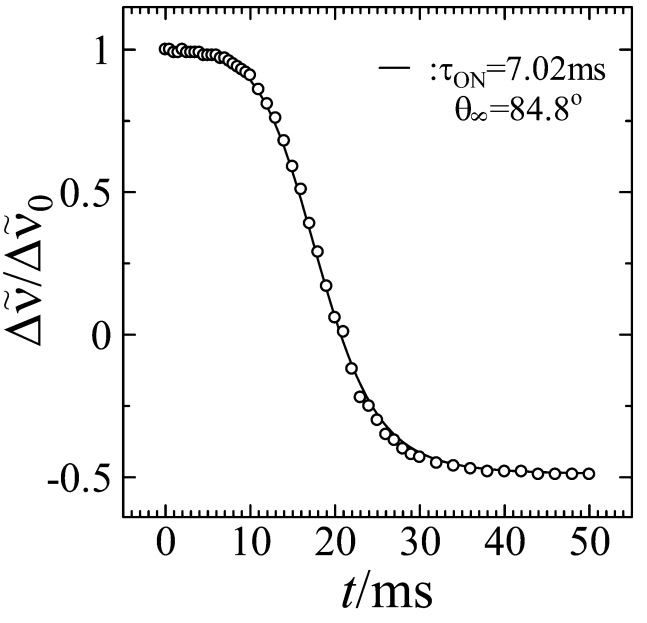

Figure 16. The turn-on alignment dynamics for 8CB-d_2 in the nematic phase at 307 K using a voltage of 84 V and 5 kHz frequency electric field applied to a 100.6 μm cell and for $\alpha=88.7^\circ$. Circles are experimental values and the solid line is the best fit to equation (2).

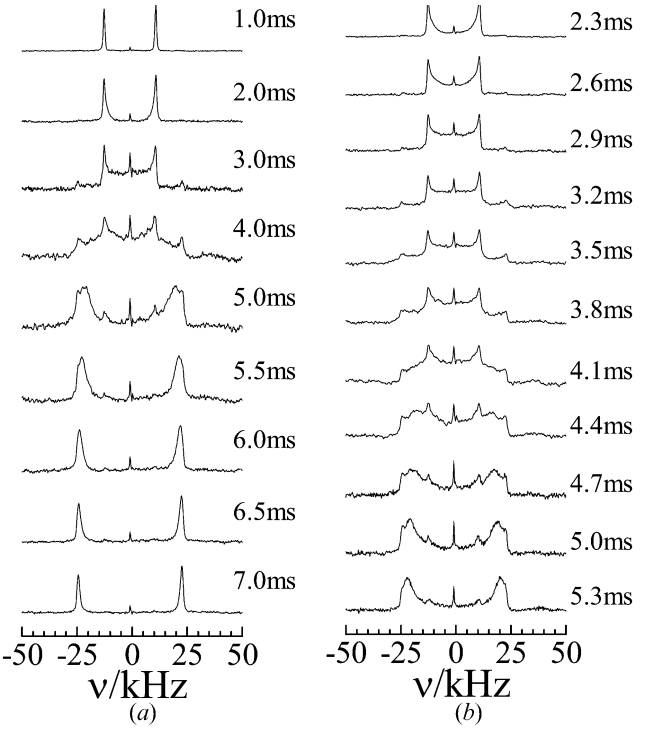

Figure 17. Typical time-resolved spectra for the turn-off alignment process for 8CB-d_2 in the nematic phase at 307 K aligned using a voltage of 100 V and 5 kHz electric field applied to a 100.6 μm cell and for $\alpha=88.7^\circ$. For (*a*) the spectra were recorded at 1 ms intervals, while for (*b*) the time step was reduced to 0.3 ms.

alignment process powder NMR spectra are observed. We confirmed the presence of powder NMR spectra by repeating the turn-off measurement between 2 and 5.5 ms at 0.3 ms steps, see figure 17 (*b*). These powder spectra are indicative of the generation of non-uniform director distributions during some stages of the alignment process before the director finally aligns parallel to the magnetic field. The non-uniform director distribution could be generated by the director orientation decreasing from its initial value at $\sim 90^\circ$, to 0°, or increasing to 180° with equal probability, i.e. by the director following two degenerate alignment pathways. This sharp contrast between the turn-on and turn-off dynamics of the nematic phase of 8CB for this geometry of $\alpha \approx 90^\circ$ is intriguing. At the moment we have no quantitative explanation for the turn-off dynamics and the contrast between the turn-on and the turn-off dynamics for 8CB. Also we have no explanation for the contrast in the behaviour of 8CB just described and that of 5CB where both the turn-on and the turn-off processes were found to follow non-uniform alignment pathways [11]. A more detailed theory than that used for the uniform director alignment is required in which not only the rotational viscosity coefficient, γ_1, is invoked but also other viscosity coefficients as well as the elastic constants which are needed when the director is not uniformly aligned during its alignment [9–11].

6. Conclusions

We have used time-resolved and time-averaged deuterium NMR spectroscopy to investigate the field-induced alignment of the nematic director in low molar mass liquid crystals such as 5CB-d_2 and 8CB-d_2. In particular we have performed deuterium NMR experiments in the presence of a.c. electric fields of varying strength and frequency, to study both the static and dynamic behaviour of the director during the alignment process. In this experimental procedure we can also control the angle, α, between the a.c. electric field and the static magnetic field and so control the possible alignment pathways of the director during changes in its orientation. In the earlier experiments, using 5CB-d_2, a high frequency (10 kHz) electric field was employed combined, in most cases, with a value of α of $\sim 45^\circ$. This resulted in uniform field-induced director alignment dynamics in which the director relaxation followed very closely the predictions of the torque-balance equation based on the Leslie–Ericksen hydrodynamic theory. This allowed the parameters $\Delta\tilde{\varepsilon}/\Delta\tilde{\chi}$ and $\gamma_1/\Delta\tilde{\chi}$ for 5CB to be evaluated with a high degree of confidence.

More recently, low frequency (several Hz to about 1000 Hz) electric fields were used in combination with two geometries. In the first geometry, the electric and magnetic fields were inclined at $\sim 50^\circ$. The torque-balance equation with a sinusoidal time dependent electric field term was solved numerically, and the predictions of the theory were confirmed experimentally from time-resolved and time-averaged deuterium NMR measurements in the nematic phase of 5CB-d_2. An oscillatory motion of the director between the electric and magnetic field directions, which is coherent over long periods of time, is observed. These director oscillations become stronger as the frequency of the electric field is lowered reaching a constant maximum at very low frequencies ($\leqslant 10$ Hz), however, they become very small at high frequencies ($\geqslant 1000$ Hz). The limiting director orientation at different frequencies can be used to provide a new, indirect route to $\Delta\tilde{\varepsilon}/\Delta\tilde{\chi}$ and $\gamma_1/\Delta\tilde{\chi}$ from the time-averaged deuterium NMR measurements.

The second geometry had the electric field essentially orthogonal to the magnetic field ($\alpha \approx 90^\circ$). For this geometry a threshold behaviour is observed for the director orientation as a function of the applied RMS voltage. The threshold voltage found for 8CB-d_2 in the nematic phase at 307 K was ~ 75 V in the 100.6 μm cell. The time-averaged spectra for this geometry were found to depend very strongly on the voltage (whether it is smaller or larger than the threshold voltage) and the frequency of the applied electric field. Most of the time-averaged spectra could be interpreted on the basis of the two values of the director orientation below and above the threshold for voltages higher and lower than the threshold voltage. However, at the threshold voltage and low frequencies (100, 40 and 30 Hz), the time-averaged spectra are very complex, possibly on account of the time-sweep of the director orientations in the threshold region. But, at a frequency of 40 Hz, the time-resolved spectra for 8CB-d_2 in the nematic phase at 307 K and at the threshold voltage of 75 V as well as at 77.5 V were all found to be essentially those characteristic of a uniform director distribution. This is surprising since this orthogonal geometry offers the possibility of degenerate director alignment pathways upon applying the electric field or turning it off; this should lead to a non-uniform director distribution and hence to the appearance of powder spectra during the oscillation in the director orientation. The complementary time-resolved turn-on and turn-off experiments for 8CB-d_2 in the nematic phase at 307 K and at high frequency (5 kHz) for this orthogonal geometry revealed more intriguing contrasts in behaviour; thus the turn-on process was found to follow a uniform path of alignment while the turn-off process was found, in marked contrast, to follow non-uniform, degenerate paths of alignment which resulted in the generation of powder spectra. We are presently unable to interpret this difference in behaviour for 8CB between the turn-on and turn-off processes or the difference in behaviour between 8CB and 5CB, where for the latter nematogen both turn-on and turn-off alignment processes were found to be non-uniform.

Acknowledgements

This work was supported by a Scientific Grant in Aid from the Japan Society for the promotion of Science (JSPS) and carried out as part of a fruitful collaboration between the Southampton and Osaka Laboratories. The authors are grateful to Professor S. Picken for valuable discussions concerning the orientation dependence of the director alignment by a field and also to Ms K. Okumoto for her help with the electric field-induced alignment experiments.

References

[1] E. Ciampi, J.W. Emsley, G.R. Luckhurst, B.A. Timimi, G. Kothe, M. Tittlebach. *J. chem. Phys.*, **107**, 5907 (1997).
[2] R.A. Wise, A. Olah, J.W. Doane. *J. Phys. (Paris)*, **36(C1)**, 117 (1975).
[3] C.J. Dunn, G.R. Luckhurst, T. Miyamoto, H. Naito, A. Sugimura, B.A. Timimi. *Mol. Cryst. liq. Cryst.*, **347**, 167 (2000).
[4] G.R. Luckhurst, T. Miyamoto, A. Sugimura, B.A. Timimi. *J. chem. Phys.*, **117**, 5899 (2002).
[5] G.R. Luckhurst, T. Miyamoto, A. Sugimura, B.A. Timimi. *J. chem. Phys.*, **116**, 5099 (2002).
[6] G.R. Luckhurst, B.A. Timimi, T. Miyamoto, A. Sugimura. *Mol. Cryst. liq. Cryst.*, **394**, 77 (2003).
[7] G.R. Luckhurst, T. Miyamoto, A. Sugimura, B.A. Timimi, H. Zimmermann. *J. chem. Phys.*, **121**, 1928 (2004).
[8] M. Bender, P. Holstein, D. Geschke. *J. chem. Phys.*, **113**, 2430 (2000).
[9] P. Esnault, J.P. Casquilho, V. Volino, A.F. Martins, A. Blumstein. *Liq. Cryst.*, **7**, 607 (1990).
[10] A.F. Martins, P. Esnault, F. Volino. *Phys. Rev. Lett.*, **57**, 1745 (1986).
[11] G.R. Luckhurst, T. Miyamoto, A. Sugimura, B.A. Timimi. *Thin Solid Films*, **393**, 399 (2001).
[12] G.R. Luckhurst, T. Miyamoto, A. Sugimura, T. Takashiro, B.A. Timimi. *J. chem. Phys.*, **114**, 10493 (2001).
[13] J.W. Emsley, J.E. Long, G.R. Luckhurst, P. Pedrielli. *Phys. Rev. E*, **60**, 1831 (1999); J.W. Emsley, G.R. Luckhurst and P. Pedrielli. *Chem. Phys. Lett.*, **320**, 255 (2000).

[14] A. Sugimura, T. Miyamoto, M. Tsuji, M. Kuze. *Appl. Phys. Lett.*, **72**, 329 (1988).
[15] G.R. Luckhurst, M. Nakatsuji, K. Okumoto, A. Sugimura, B.A. Timimi, H. Zimmermann. *Mol. Cryst. liq. Cryst.*, **398**, 235 (2003).
[16] A.M. Kantola, G.R. Luckhurst, B.A. Timimi, A. Sugimura. *Mol. Cryst. liq. Cryst.*, **402**, 117 (2003).
[17] G.R. Luckhurst, A. Sugimura, B.A. Timimi, H. Zimmermann. *Liq. Cryst.* (2005).
[18] D.A. Dunmur, M.R. Mansfield, W.H. Miller, J.K. Dunleavy. *Mol. Cryst. liq. Cryst.*, **45**, 127 (1978).
[19] G.R. Luckhurst, K. Okomoto, A. Sugimura, B.A. Timimi. Unpublished results.

APPENDIX

Uniform and non-uniform director alignment

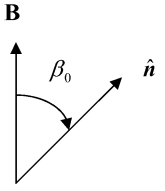

If a field is applied at an angle β_0 to the director will this align it uniformly or could different directors move in opposite directions? For the latter to occur the energy gained by a decrease in β must compensate for the loss in energy resulting from an increase in β. The anisotropic magnetic energy is given by

$$U = -\mu_0^{-1}\frac{\Delta\tilde{\chi}\,\mathbf{B}^2}{3}P_2(\cos\beta) \tag{A1}$$

when the director makes an angle β with the field. This energy is now expanded for small deviations from β_0 using a Taylor series up to second order. The gradients needed for this are

$$\frac{\mathrm{d}P_2(\cos\beta)}{\mathrm{d}\beta} = -3\cos\beta\sin\beta = -\frac{3}{2}\sin 2\beta \tag{A2}$$

$$\frac{\mathrm{d}^2P_2(\cos\beta)}{\mathrm{d}\beta^2} = -3\cos 2\beta. \tag{A3}$$

The energy when β increases from β_0 by $\delta\beta$ is

$$U(\beta_0+\delta\beta) = -\mu_0^{-1}\frac{\Delta\tilde{\chi}\,\mathbf{B}^2}{3}\times \times\left\{P_2(\cos\beta_0) - \frac{3}{2}\sin 2\beta_0\delta\beta - \frac{3}{2}\cos 2\beta_0\delta\beta^2\right\} \tag{A4}$$

i.e. both the linear and quadratic terms cause the magnetic energy to increase, as expected. When the angle decreases by $\delta\beta$ the new energy is

$$U(\beta_0-\delta\beta) = -\mu_0^{-1}\frac{\Delta\tilde{\chi}\,\mathbf{B}^2}{3}\times \times\left\{P_2(\cos\beta_0) + \frac{3}{2}\sin 2\beta_0\delta\beta - \frac{3}{2}\cos 2\beta_0\delta\beta^2\right\}. \tag{A5}$$

Now the linear and quadratic terms have opposite signs but the linear term which should be bigger is positive, so decreasing the overall energy. When both changes ($\delta\beta$ and $-\delta\beta$) take place then the total change in energy is

$$U(\beta_0\pm\delta\beta) = -\mu_0^{-1}\frac{\Delta\tilde{\chi}\,\mathbf{B}^2}{3}\times \times\left\{P_2(\cos\beta_0) - 3\cos 2\beta_0\delta\beta^2\right\}. \tag{A6}$$

The linear term has vanished and the sign of the quadratic term is controlled by that of $\cos 2\beta_0$. If $\beta_0 \leqslant 45^\circ$ then $\cos 2\beta_0$ is positive which means that the magnetic energy increases, the system is more unstable and so both fluctuations ($\pm\delta\beta$) cannot occur. In other words the director can only move in one direction. For $\beta_0 > 45^\circ$, $\cos 2\beta_0$ is negative, the magnetic energy decreases and both fluctuations occur.